ELSEVIER

Materials Science and Engineering C 23 (2003) 23–31

MATERIALS SCIENCE & ENGINEERING C

www.elsevier.com/locate/msec

Nanoimprint lithography: an alternative nanofabrication approach

C.M. Sotomayor Torres[a,*], S. Zankovych[a], J. Seekamp[a], A.P. Kam[a], C. Clavijo Cedeño[a], T. Hoffmann[a,1], J. Ahopelto[b], F. Reuther[c], K. Pfeiffer[c], G. Bleidiessel[c], G. Gruetzner[c], M.V. Maximov[d], B. Heidari[e]

[a] *Department of Electrical and Information Engineering, Institute of Materials Science, University of Wuppertal, Gauss-Strasse 20, D-42097 Wuppertal, Germany*

[b] *VTT Centre for Microelectronics, P.O. Box 1208, FIN 02044 VTT, Finland*

[c] *Micro-Resist Technology GmbH, Koepernickerstr. 325, D-12555 Berlin, Germany*

[d] *A F Ioffe Physical-Technical Institute, St. Petersburg, Russia*

[e] *Obducat AB, Geijersgatan 2A, P.O. Box 580, SE-01 25 Malmö, Sweden*

Abstract

A status report of nanoimprint lithography is given in the context of alternative nanofabrication methods. Since the ultimate resolution of nanoimprint appears to be determined by the stamp, this is discussed in detail, particularly the recent developments on polymer stamps. The scope of the technique is illustrated with applications in passive optical structures and organic devices. Throughout the report, critical dimensions are discussed, as well as other challenges facing nanoimprint lithography.

Keywords: Nanofabrication; Nanoimprint lithography; Polymer moulding

1. Introduction

Progress in nanotechnology demands the capability to fabricate nanostructures in a variety of materials with an accuracy in the nanometre scale and sometimes in the atomic scale. Stringent nanofabrication specifications have to be met in industrially relevant processes due to manufacturability and costs considerations as, for example, in the electronics industry. However, less demanding conditions are needed for developments in optics, sensors and biological applications. In a laboratory environment, at the level of enabling nanofabrication techniques as tools for experiments to understand the underlying science and engineering in the nanometre scale, easily accessible and flexible nanofabrication approaches are required for investigations in, e.g., materials science, organic optoelectronics, nano-optics and life sciences. Alternative techniques to cost-intensive or limited-access fabrication methods with nanometre resolution have been under development for nearly two decades. One clear example is the evolving set of scanning probes techniques, which has become ubiquitous in many research areas. If one considers planar structures, i.e., where nanostructuring is carried out on a surface, as distinct from a three-dimensional nanofabrication or multilayer self-assembly, then several emerging nanofabrication techniques can be discussed. Their classification depends on whether the nature of the patterning is chemical or physical, or its modality in time is parallel or sequential, or a hard or a soft mould or stamp is used, etc. The literature on the subject is increasing very rapidly and recent reviews on, for example, progress in micro-contact printing [1,2], scanning probe-based techniques [3] and nanoimprint-based lithography (NIL) technique [4], have been published. Recent developments in nanopatterning include dip pen lithography [5] and nanoplotting [6], as well as stenceling [7].

In this paper, we concentrate on nanoimprint lithography [8] partly as a potential cost-efficient parallel nanofabrication technique and as a way to realise simple devices in a single patterning step. What follows is a brief description of nanoimprint lithography that is given and compared to other emerging nanofabrication approaches. Since the resolution depends on the stamp, issues around stamp fabrication are discussed. To illustrate the potentials of the techniques,

* Corresponding author: Tel.: +49-202-439-2920; fax: +49-202-439-3037.

E-mail address: clivia@uni-wuppertal.de (C.M. Sotomayor Torres).

[1] Present address: Inter-university Centre of Microelectronics, B-3001 Leuven, Belgium.

0928-4931/02/$ - see front matter © 2002 Elsevier Science B.V. All rights reserved.
PII: S0928-4931(02)00221-7

some applications are described. A discussion of the remaining challenges facing nanoimprint lithography to become accepted as a parallel process follows. A view on perspectives of nanoimprint lithography concludes this manuscript.

2. Nanoimprint lithography

To nanoimprint a surface, three basic components are required. These are: (i) a stamp with suitable feature sizes fabricated by, for example, electron beam lithography and dry etching, if features below 200 nm are needed or, by optical lithography for larger features. (ii) The material to be printed, usually a layer of polymer of a few hundred nanometres' thickness with suitable glass transition temperature T_g and molecular weight, spun of a substrate and (iii) equipment for printing with adequate control of temperature, pressure and control of parallelism of the stamp and substrate. In essence, the process consists of pressing the stamp using a pressure in the range of about 50–100 bar, against the thin polymer film. This takes place when the polymer is held some 90–100 °C above its T_g, in a time scale of a few minutes, during which the polymer can flow to fill in the volume delimited by the surface topology of the stamp. The stamp is detached from the printed substrate after cooling both the stamp and substrate. This takes place in a cycle involving time, temperature and pressure. In Fig. 1, the schematic of the NIL process is shown, as well as a characteristic temperature and pressure cycle.

NIL has the advantage over conventional nanofabrication methods, of being a flexible, low-cost and biocompatible fabrication technique. There are several variations of NIL including the most popular parallel process using wafer size stamps [9], a sequential process called Step-and-Stamp Imprint Lithography (SSIL) [10] and roll-to-roll NIL [11].

There are several key achievements in the development of NIL as a nanofabrication technique and its potential applications reported over the last 7 years. These are mentioned in a chronological sequence. (a) The first report of what is known as NIL as a potential nanofabrication technique appeared in 1995 [8]. (b) Feature sizes down to 6 nm by NIL are achieved in 1997 [12] in PMMA. (c) The use of NIL to fabricate polymer-based optical devices is demonstrated in 1998 [13]. (d) Alignment accuracy of 1 μm is demonstrated using commercially available equipment [14]. (e) In 1999, Yu et al. [15] reported on NIL-made metal-semiconductor-metal MSM photodetectors with no mobility decrease up to NIL pressures of 600 psi. (f) Broadband waveguide metal polarisers with 190 nm period were reported by Wang et al. [16]. (g) NIL of 150 mm diameter wafers is achieved [9]. (h) A sequential variation of NIL, step-and-stamp imprint lithography is demonstrated using a commercial flip-chip bonder [10]. (i) Polymers developed specifically for NIL [17] become commercially available in 2000 (mr-I-8000 and mr-I-9000). (j) Low-cost stamp replication using NIL is demonstrated [18]. (k) Mäkela et al.[19] showed that the electrical conductivity of nanoimprinted conducting polymers is not

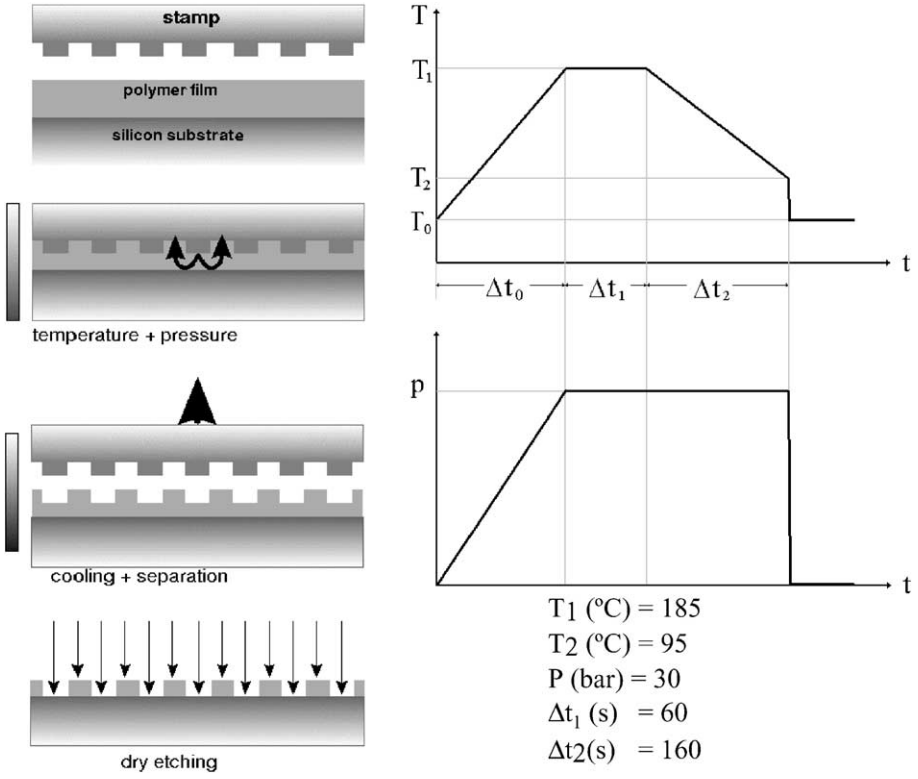

Fig. 1. Schematics of the nanoimprint lithography process (left) and of the temperature–pressure temporal sequence (right). The inset shows typical process parameters.

impaired by imprint lithography. (l) A new resistance suitable for NIL, which is also sensitive to electron beam and UV lithography, was reported [20]. (m) The first microfluidic device made by NIL is reported by Studer et al. [21] in 2001. (n) An anti-adhesion treatment for stamps containing sub-100 nm features is reported [22]. (o) A quality control method with in situ potentials for NIL based on optical microscopy is successfully tested in the laboratory [23]. (p) Applications of NIL to realise two-dimensional photonic crystals have been recently reported [24,25]. Automated equipment for NIL is currently available from, e.g., Obducat and Electrovision. For the laboratory scale, simple hydraulic presses are suitable.

The precise process parameters of a NIL cycle depend on the target application, since issues arising with respect to fabrication capabilities vary for different applications. For example, if NIL were to become a serious contender for the fabrication of electronic devices with feature sizes close to 10 nm, overlay accuracy for multilevel fabrication and throughput, the 80 wafers per hour benchmark, would have to be addressed. It represents almost non-surmountable barriers, given the current status of NIL. For one-level lithography, for example, to produce an etch mask, NIL has proven capable of printing on polymers which offer selectivity for dry etching [26]. Likewise, when a polymer film is patterned to contain a particular relief for use as a grating. Nevertheless, NIL has to meet a number of demands before it becomes the choice for one-level nanofabrication where critical dimensions are needed. For example, it has become clear that nanorheology plays a key role when printing on thin polymer films and when both very large and very small features are present in the stamp [27]. This is discussed in Section 5 below.

3. Stamp fabrication

In first approximation, the ultimate resolution of NIL depends on the minimum feature size in the stamp. For high-resolution stamps, they are usually made by electron beam lithography and dry etching, and for shallow stamps, by metal lift-off. The material of choice is Si or SiO_2, which is sometimes electroplated. Depending on application, stamps in wafer-size scale have been studied by several groups. The stamp design is intrinsically correlated to the polymer to be printed. Polymer flow in NIL has been studied in PMMA [28] and other printable polymers [29] and reviewed in Ref. [4]. The flow under NIL conditions has been found to depend on the molecular weight of the polymer to be printed and, more importantly, on the rate of application of both pressure and temperature. This is not surprising, given the variation of polymer viscosity over several orders of magnitude around the glass transition temperature. Thus, the viscoelastic properties of the printable polymer, the stamp design and the process parameters, determine the thickness of the polymer the residual layer (see Ref. [4] for a review). However, it remains a non-trivial problem to model it in order to facilitate the design of stamps with a complex mixture of features and

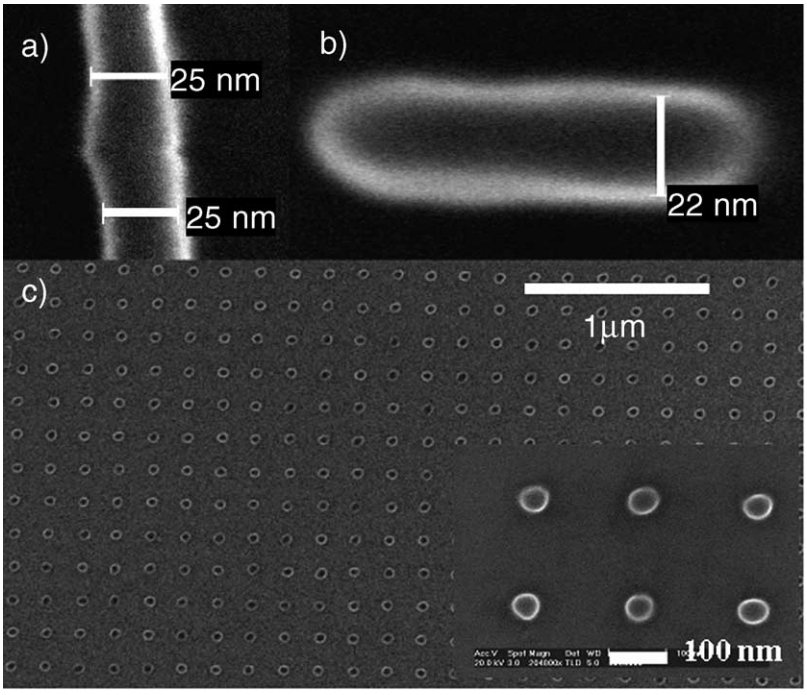

Fig. 2. SEM micrograph of patterns written by electron beam lithography on mr-L 6000 (see text) spun on Si, after development: a wire of 25 nm width (a), a dash of 22 nm (b) and an array of dots of 50 nm diameter (c).

patterns. While this can be calculated to various degrees of accuracy, an additional uncertainty is introduced when the residual polymer layer is removed in an oxygen plasma process. Since the space between the printed features increased with a size variation of several nanometres [30], depending on the residual layer thickness to be removed and, presumably, the feature size. These aspects then contribute to complicate the issue of critical dimensions.

Metal stamps with features smaller than 10 nm have been fabricated by electron beam roughness and lift-off. However, the metal roughness was found to be a problem for sizes below 10 nm due to the granularity of the evaporated metal.

A promising development, with potential impact in a range of applications, is the syntheses of a new polymer, such as mr-L6000, developed by Micro-Resist Technology. This particular polymer is suitable for NIL and at the same time is UV- and electron beam-sensitive [20]. mr-L6000 has high electron sensitivity, ~ 5 μC/cm2 compared to 80–200 μC/cm2 for PMMA, which results in shorter electron beam writing times. The limits of its resolution are still not found and currently these are around 20 nm. An example is shown in Fig. 2, where several patterns were written by electron beam. After development, the features are very smooth. This polymer can be nanoimprinted. In Fig. 3 AFM images of a stamp and a print using mr-L 6000 are shown with lateral dimensions of 40 and 30 nm high. To obtain this pattern on the stamp by electron beam lithography, 100 nm of the polymer were spun and exposed to 30 kV at 5 μC/cm2, developed for 30 s, exposed to UV illumination for 2 min and finally, hard baked at 120 °C for 5 min. NIL was performed on a layer of 100 nm thickness at $T_{impr} = 100$ °C, a pressure of 40 bar for 2 min, and separation of stamp and printed substrate at $T_{sep} = 30$ °C. More details, a comparison of cross-linkable and further examples can be found in Ref. [31]. Moreover, the appeal of this material is its suitability for mix-and-match lithography with applications in MEMs, NEMs and microfluidics, to name but a few.

The need to keep the stamp parallel to the substrate during the process is an essential condition to obtain uniform thickness of the residual layer and the patterned features across the sample area. Likewise, thermal gradients must be avoided using suitable heating and cooling elements. These thermomechanical aspects are incorporated in the design of nanoimprint lithography equipment. Other relevant aspects concerning stamp size, adhesion, curing, cleaning and lifetime, which determine throughput, have been discussed elsewhere [32].

4. Examples of nanoimprint lithography applications

4.1. Optics

One obvious application of NIL is the replication of periodic features in the submicron regime, such as passive optical devices, including the fabrication of polymers suitable for the 1.5 μm communications wavelength range. Metal gratings [16], submicrometer electrodes [15], polymer gratings [25] are some of the structures which have already been realised and some have been commercialised by, e.g., Nano Opto (Somerser, N.J., USA).

With respect to gratings, a 25 mm^2 uniform grating has been realised in a single print with feature sizes of 400 nm [25]. The efficiency of the grating was below that of commercially available ones, depending on polarization, but its profile was better than those defined by holography and was probably better than ruled gratings, due to the anisotropic etching of the stamps. Using Si stamps made by optical interference lithography in conjunction with dry and wet etching of SiO_2 and Si_3N_4 and transferring the 100 nm pitch grating by NIL onto a polymer to act as mask for pattern transfer. The final structure was a 100 nm Si grating, i.e., a subwavelength, which the authors suggest, have applications in devices based on form birefringence [33]. What remains to

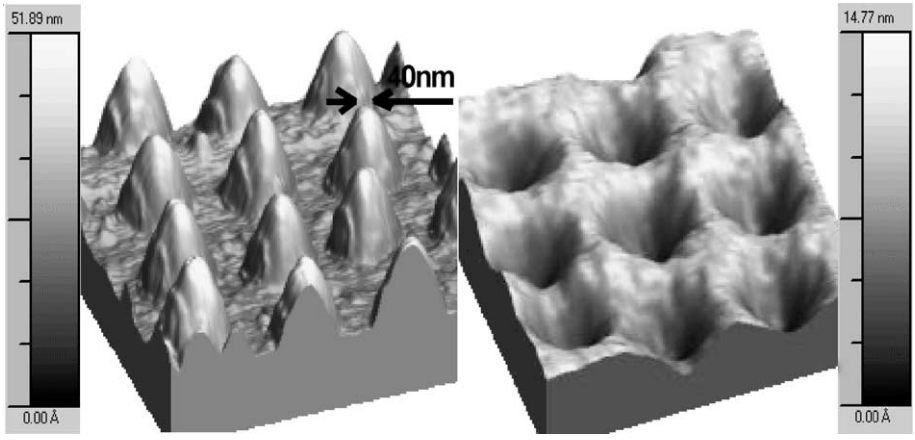

Fig. 3. AFM images of a stamp made out of mr-L 6000 (see text) by electron beam lithography with top diameter of 40 nm, base diameter of 100 nm and 30 nm high; (left) and a print into mr-L 6000 (right).

be quantified are grating ghosts and anomalies. On the other hand, the prospect of realising curved gratings is appealing, in particular, considering Teflon as the grating material. In general, it is essential that optical properties of the polymer remain unchanged after fabrication and during its lifetime to avoid changes of the absorption and/or the refractive index. While feature sizes for grating application in the visible are somewhat relaxed, polymer structures feature sizes below 50 nm, whether periodic or not, have to be treated with caution due to the elastic relaxation which can occur over periods from days to years.

Critical dimensions depend on applications and NIL is put to the test in one of the most demanding applications, namely, the fabrication of one-dimensional and two-dimensional photonic crystals, such as photonic crystal waveguides [25], ultra-refractive elements and optical microcavities. In some materials, the critical dimension required is better than 10 nm. Depending on the role of the passive structure, the control of the minimum lateral feature size (critical dimension) can be as demanding as a few nanometres.

The applications of NIL in optics are not limited to passive structures. The possibility to pattern a mask with NIL as it is done with electron beam lithography, and subsequently, etching the substrate material to transfer the pattern into an optically active layer, and is also a very attractive avenue. In particular, as optical devices increasingly require submicron features, the need for cost-efficient lithography increases. In this respect, one issue to be addressed is whether the NIL cycle, in particular the pressure parameter, induces non-radiative recombination centres, thereby, potentially limiting the radiative lifetime of a structured light-emitting diode or semiconductor laser. To this effect, a silicon stamp containing parallel wires with 800 nm period was used to print PMMA spun on GaAs. After lift-off, the wire pattern was transferred to a GaAs substrate resulting in 200 nm ribs [34] as shown in Fig. 4. While this proves that printed PMMA using NIL can be used as a mask, this is a preliminary result and several aspects need to be revisited, especially the wire width changes from stamp, through lift-off and the dry etching step. Some aspects may have a clear path, for example, other polymers with higher resistance to dry etching can be used. These so far, have been tested in the typical dry etching gas mixture for silicon and not for GaAs. This remains to be done. Once the quality of the printed etch mask is improved, the change in lateral size during oxygen plasma etching of the nanoimprinted window to remove the residual layer also needs to be better understood and controlled, and eventually be considered in the stamp design for a given process. The emission from these GaAs wires is currently under study.

In a parallel experiment to determine if NIL results in optically relevant damage of the underlying semiconductors, photoluminescence and photoluminescence excitation (PLE) spectroscopy was carried out at 20 K on multiple quantum well samples before and after NIL. The samples had quantum wells of different thicknesses as different depths from the surface to be imprinted. Two aspects were investigated: the integrated photoluminescence intensity and the emission energy and in PLE, the changes of strain in the quantum wells. Two types of quantum wells were examined: GaAs-GaAlAs and GaInAs-InP, one having quantum wells as a compound structure and the other an alloy. The full experimental details are given elsewhere [35]. The findings are very encouraging in that, using Si stamps, printing temperatures up to 190 °C and applying pressures up to 200 bar for 5 min resulted in no detectable change in the emission energy nor in the integrated emission intensity. The PLE data from the GaAs-GaAlAs and

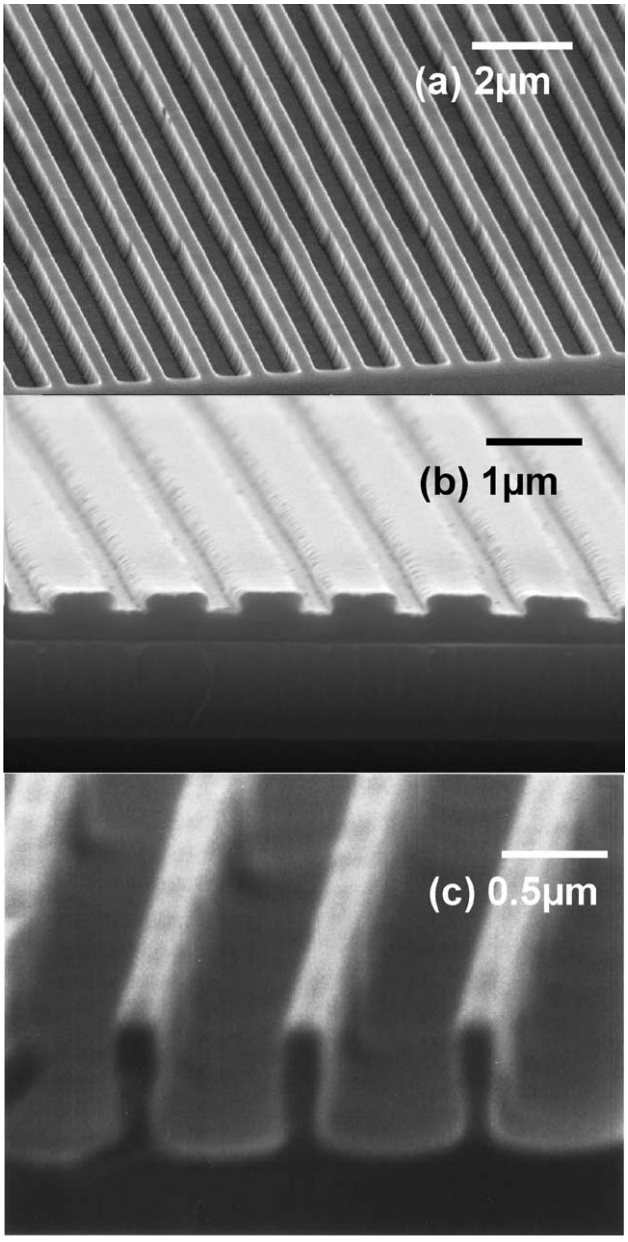

Fig. 4. SEM micrographs of: (a) the Si stamp with 800 nm period used to print the structure in (b); (b) printed PMMA on GaAs and (c) GaAs wires after dry etching using PMMA NIL patterning and lift-off, the wire width is approximately 200 nm.

the GaInAs-InP quantum wells showed no evidence of strain as no changes were detected in the splitting of the heavy hole and light hole excitons after printing at a pressure of 200 bar.

Thus, samples subjected to NIL show that their low-temperature integrated emission, emission energy and strain are not affected. This means that once the critical dimension issue is overcome, NIL has the potential to replace electron beam lithography to write masks for semiconductor optoelectronic devices.

Based on developments to produce high aspect ratio (1:20) hard stamps based on SiC for printing thin aluminium film [36], the NTT team has shown that a silicon carbide stamp can be used to nanoimprint a thin organic layer with a two-dimensional photonic crystal structure [24].

It is clear that much remains to be done and the potential to nanoimprint hybrid optical circuits is there.

4.2. Organic optoelectronics

NIL is a natural fabrication approach for organic optoelectronics and sensors. In addition to useful optical device structures printed in a single step in layers containing the small molecule Alq_3 as an example of a patterned light-emitting organic layer [13]. PMMA and in polystyrene for gratings and one-dimensional photonic crystal structures [25] and the study of conductivity in printed polyaniline blend [19], other reports on NIL for organic layers have appeared. In particular, printing patterns of nanoelectrode arrays down to 100 nm into oligomers, such α-sexithyo-

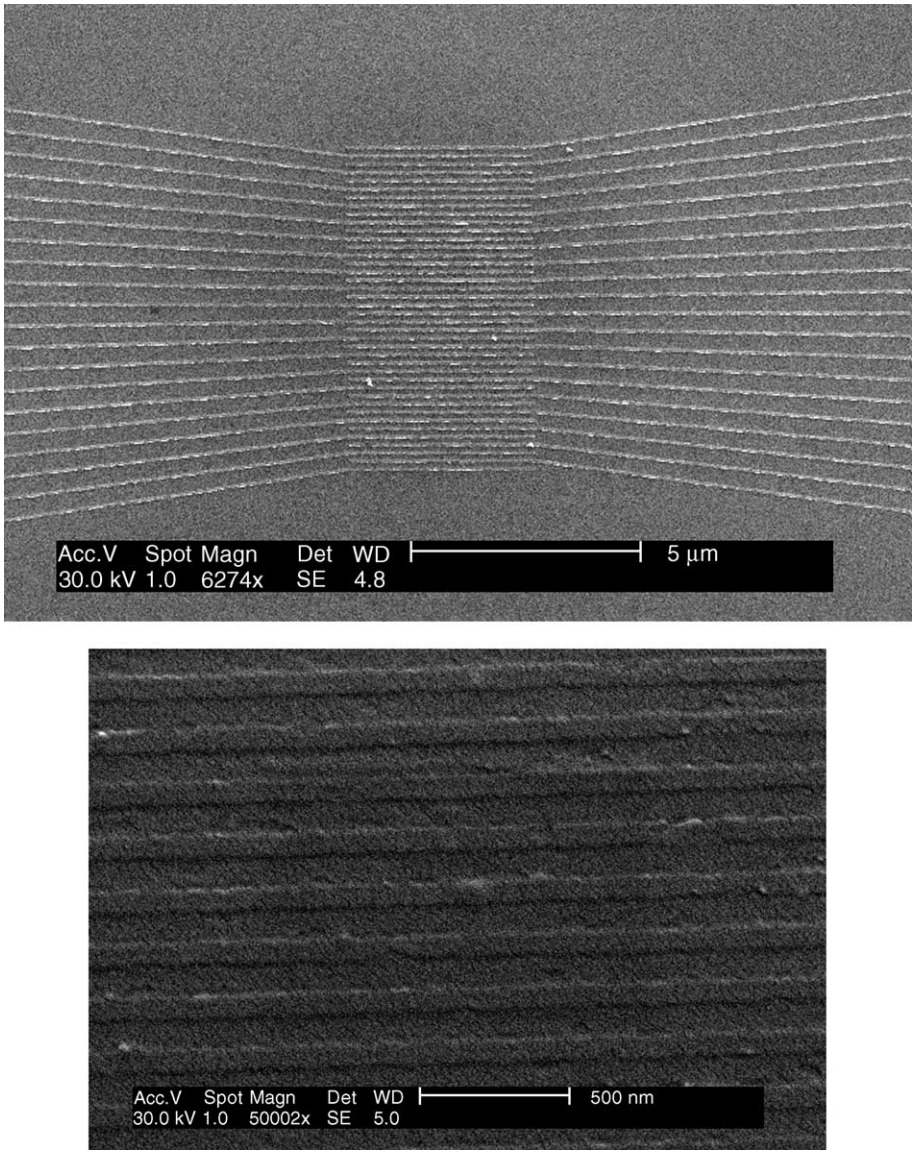

Fig. 5. SEM micrographs of (top) part of an electron beam written stamp after Au and Ti lift-off containing an interdigitated nanoelectrode array overlapping over 4 μm and having channel length of 90 nm and (bottom) a section of the printed 950 K molecular weight PMMA.

phene, [37] and of UV curable oligomers in low-temperature NIL, such as the modified triphenylamine analogues PDAS and PBAS, into structures which, after patterning, still retain their conducting character [38]. Organic thin film transistor (OTFT) structures based in pentacene have been made with features down to 100 nm and their electrical characteristics measured in a NIL process combined with cold welding [39], as well as using the standard NIL process [40]. The cold welding approach has the advantage of reducing surface contact contamination, which is a main problem in the fabrication of organic electronic devices. In Fig. 5, SEM micrographs of part of an electron beam written stamp after Au and Ti lift-off containing an interdigitated nanoelectrode array overlapping over 4 μm in the central part and having channel length of 90 nm. A section of the nanoimprinted 950 K molecular weight PMMA is also shown. This process is now being applied to oligomers for thin film transistors [40].

One aspect, which dramatically affects the fabrication of thin film transistors with nanometre electrodes, is packaging. One approach to the lateral OTFT could be to bond two substrates, one with the spun conducting organic layer on one side and one half of the package, while the other would have on one side the source and drain electrode arrays connected to the package via vias. This concept, so far to be tested for contamination and viability, is illustrated in Fig. 6.

The attractive feature of organic optoelectronics is the prospect of having both optical and electronic devices on a single platform. However, much engineering, science and testing and design work lays ahead for structures with feature sizes close to 50 nm.

4.3. Other applications

Other applications of NIL are in the area of nanomagnetism [41] and data storage [42], however, molecular electronics [43], microfluidics [21], and bioelectronics [44], to name but a few. The combination of NIL with other techniques also lends itself to many potential applications.

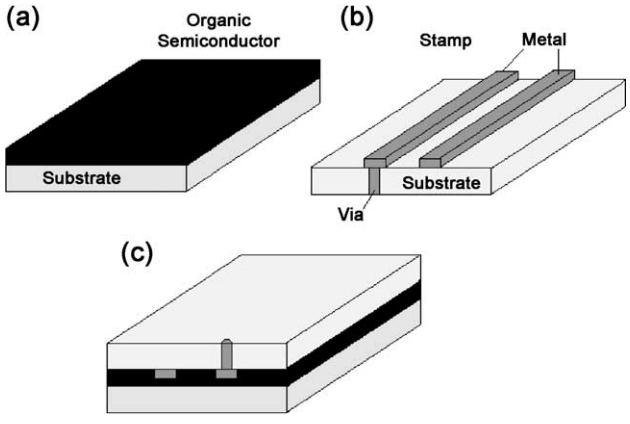

Fig. 6. Schematics of an approach to realize lateral OTFT and addressing the packaging problem.

5. Some roadblocks

One of the criticisms levied at NIL is the *multilevel issue*. For this to be overcome, the first step is to find engineering solutions for x–y in-plane alignment to control overlay to, ideally, better than 10 nm. In general, the stamp is considered the functional equivalent of the photo-mask in conventional projection lithography. At present, the limit is $\sim$ 1 μm with a standard deviation of 0.4 μm over a 100 mm wafer using a commercially available aligner [45]. Upon first approximation, alignment depends on stamp size, the thermal and mechanical stability of the equipment and polymer during alignment and the choice of stamp and substrate material. A compromise may be found in applications with few lithography and mask steps for specific applications. Other factors and possible solutions have been discussed in Refs. [4,32].

The other key aspect is *throughput*. This is heavily dominated by cost and comparisons and usually made to the microelectronic industry with its 80 wafers per hour yardstick. Whereas, a working definition of throughput in NIL as understood in conventional lithography is still lacking, a rough approximation would consider the actual printing time, loading, alignment and separation times, which currently add up to 10–15 min. Factors contributing to throughput includes, the stamp size, high density of features, absence of an anti-adhesive layer, polymer curing time, printing temperature and pressure and stamp lifetime, among others. One figure of merit used when discussing nanofabrication techniques is the "exposure rate", which for nanoimprinting is about 0.152 cm^2/s to print for 10 nm features over a 150 mm wafer in 20 min including heating and cooling cycles.

As any other technology coming under what is generically known as printing, NIL must face up to validation and standards. *Validation*, or the quality control issue, needs agreement as to what counts as tolerances for a good print, whereas *standards* depend strongly on design rules and it is too early to expect definitive statements.

Concerning quality control, one pioneering approach for potential online quality control of stamp damage and/or adhesion is based on optical microscopy of fluorescent dye loaded printable polymers [23]. Preliminary tests show that the presence of particles down to 100 nm can be detected while tracking the status of the stamp. By recording the complementary fluorescence image, the status of the printed substrate can be obtained. Optical microscope images are loaded digitally for fast image processing.

The problem of critical dimension is one that, depending on the fabrication demands below 50 nm, can become a serious bottleneck for NIL. Studies using electron beam-sensitive resistance for NIL have shown that good CD control can be obtained in highly dense patterns with feature size down to about 75 nm [46]. Factors affecting CD control include the glass transition temperature of the polymer, as well as its long-term viscoelastic properties. The design has to incorporate polymer shrinkage in temporal and thermal

process steps, e.g., when the residual layer is removed, which affects the final size of the printed features. Below the 20 nm range, the polymer properties themselves come into play with relaxation taking place over weeks and months affecting not only the morphology but also the depth and/or aspect ratio of the printed features. Here is where combinatory fabrication approaches involving NIL and polymer development have a role to play. In particular, the use of polymers, which lend themselves to be modified by electron beams, UV exposure and NIL.

6. Status and perspectives

At an international workshop on NIL and related techniques held in Lund in January [47], the participants produced a table with the status on some alternative nanofabrication techniques. An updated version is shown in Table 1, which includes the recent report of laser-assisted NIL for ultra-fast silicon [48].

It can be safely argued that NIL for nanoelectronics needs to demonstrate multilevel capabilities. However, simpler applications, which encompass magnetic arrays, biosensors, passive optical elements, MSM detectors, etc., do not have the strong overlay demand. Patterning in three dimensions, akin to using SU8, will lead to extensions to three-dimensional micro- and nanosystems by using multilayers of suitable printable polymers, which are also sensitive to UV and electron beams.

However, in order to realise many of the potentials of NIL efforts need to be made towards automation and alignment down to tens of nanometres and over 180 mm wafers. Much remains to be understood, especially the viscoelastic properties of very thin polymer layer in order to make progress on standards and critical dimension control, which necessarily pass through adequate design of the stamp features. Nevertheless, the versatility of the NIL process requires the qualification of CD control with respect to a particular application. This means that we can expect further developments in, for example, optically active polymers suitable for printing. Looking ahead at low-cost options for subwavelength scale replication of plastic optical elements and circuits, NIL appears very attractive as a technology to fabricate wavelength demultiplexers in polymers as well as photonic crystals. As nanotechnology developments increasingly need accessible nanofabrication techniques, NIL is posed to become an obvious choice for many public and private laboratories as well as production companies.

Acknowledgements

This work is partly supported by the EU IST FET project CHANIL (IST-1999-13415), EU Growth project MONALISA (GRD-2000-25592), the EU IST project APPTech (IST-2000-29321), the German Research Council (DFG) and the INTAS project 99-009928. We are indebted to our project partners for many illuminating discussions. CMST

Table 1
Comparison of printing and related techniques

Process	Process type	Minimum feature, minimum pitch (nm)	Combined large and small features	Largest area printed	Overlay accuracy	Time for alignment, printing, release, cycle time	Number of times stamp was used
Imprint	Nano imprint[a]	6–40	10 nm/100's μm	100 mm wafer	0.5 μm[b]	a few minutes; 10 s; a few minutes; 10–15 min	50
	Step-and-Stamp[c]	300–600	300 nm/100's μm	150 mm^2	1 μm	1 min; 5 min; a few seconds.; 6 min/step	36
	Step and flash[d]	10–50	20 nm–mm	1 inch; wafer	1 μm	1 min; 10–20 s; 10 s; 5 minute/flash	>100 without clean
Printing	Micro-contact printing[e]	60–200	60 nm/60 mm	12 in. wafer	0.5–1 μm	1 min; 1–30 s; 10 s; 2 min	>100
Stenciling	Shadow[f,g]	10	10 nm/10's μm	From 50 μm^2–1 mm^2 [g]	–	a few minutes; 15 min; a few minutes; 30 min	–
Combined Techniques	UV Lith + NIL[h]	100	100 nm-contact pads	400 μm^2	1 μm	–	–
	Laser-assisted NIL[i]	10	140 nm	10 nm–10's μm	2.3 mm^2	250 ns	–

Modified from Ref. [46].
[a] Ref. [8].
[b] S.Y. Chou, private communication.
[c] J. Ahopelto, private communication.
[d] H. Kurz, private communication.
[e] Ref. [1].
[f] Ref. [49].
[g] Ref. [7].
[h] Considering imprint first followed by UV photolithography.
[i] Ref. [48].

would like to thank Dr. Y. Cheng (CNRS-LPN), for his help in compiling Table 1.

References

[1] B. Michel, A. Bernard, A. Bietsch, E. Delamarche, M. Geissler, D. Juncker, H. Kind, J.-P. Renault, H. Rothuizen, H. Schmid, P. Schmidt-Winkel, R. Stutz, H. Wolf, IBM J. Res. Develop. 45 (2001) 697.
[2] Y. Xia, X.-M. Zhao, G.M. Whitesides, Microelectron. Eng. 32 (1996) 255–268.
[3] P. Vettiger, et al., Microelectron. Eng. 46 (1–4) (1999) 101.
[4] H.-C. Scheer, H. Schulz, T. Hoffmann, C.M. Sotomayor Torres, in: H.S. Nalwa (Ed.), Handbook of Thin Film Materials, vol. 5, Academic Press, New York, USA, 2002, pp. 1–60.
[5] D. Pinner, J. Zhu, F. Xu, S. Hong, Science 283 (1999) 661–663.
[6] S. Hong, C.A. Mirkin, Science 288 (2000) 1808–18011.
[7] J. Brugger, J.W. Berenschot, S. Kuiper, W. Nijdam, B. Otter, M. Elwenspoek, Microelectron. Eng. 53 (2000) 403.
[8] S.Y. Chou, P.R. Krauss, P.J. Renstrom, Appl. Phys. Lett. 76 (1995) 3114.
[9] B. Heidari, I. Maximov, E.-L. Sarwe, L. Montelius, J. Vac. Sci. Technol., B 18 (2000) 3552–3556.
[10] T. Haatainen, J. Ahopelto, G. Gruetzner, M. Fink, K. Pfeiffer, Proc. SPIE 3997 (2000) 874–880.
[11] H. Tan, A. Gilberston, S.Y. Chou, J. Vac. Sci. Technol., B 16 (1998) 3926.
[12] S.Y. Chou, P.R. Krauss, W. Zhang, L. Guo, L. Zhuang, J. Vac. Sci. Technol., B 15 (1997) 2897.
[13] J. Wang, X. Sun, L. Chen, S.Y. Chou, Appl. Phys. Lett. 75 (1999) 2767.
[14] A. Lebib, Y. Chen, J. Bourneix, F. Carcenac, E. Cambril, L. Couraud, H. Launois, Microelectron. Eng. 46 (1999) 319.
[15] Z. Yu, S.J. Schablitsky, S.Y. Chou, Appl. Phys. Lett. 74 (1999) 2381.
[16] J. Wang, S. Schablitsky, Z. Yu, W. Wy, S.Y. Chou, J. Vac. Sci. Technol., B 17 (1999) 2957.
[17] K. Pfeiffer, G. Bleidiessel, G. Gruetzner, H. Schulz, T. Hoffmann, H.-C. Scheer, C.M. Sotomayor Torres, J. Ahopelto, Microelectron. Eng. 46 (1999) 431 (See also http://www.microresist.de).
[18] H. Schulz, D. Lyebyedyev, H.-C. Scheer, K. Pfeiffer, G. Bleidiessel, G. Gruetzner, J. Ahopelto, J. Vac. Sci. Technol., B 18 (2000) 3582.
[19] T. Mäkela, T. Haatainen, J. Ahopelto, H. Isolato, J. Vac. Sci. Technol., B 19 (2001) 487.
[20] K. Pfeiffer, M. Fink, G. Aherens, G. Gruetzner, F. Reuther, J. Seekamp, S. Zankovych, C.M. Sotomayor Torres, I. Maximov, M. Beck, M. Grazcyk, L. Montelius, H. Schulz, H.-C. Scheer, F. Steingrueber, Microelectron. Eng. 61–62 (2002) 393.
[21] V. Studer, A. Pépin, Y. Chen, Appl. Phys. Lett. 80 (19) (2002, May 13).
[22] M. Beck, M. Graczyk, I. Maximov, E.-L. Sarwe, T.G.I. Ling, M. Keil, L. Montelius, Microelectron. Eng. 61–62 (2002) 441.
[23] C. Finder, M. Beck, J. Seekamp, K. Pfeiffer, P. Carlberg, I. Maximov, F. Reuther, E.-L. Sarwe, S. Zankovych, J. Ahopelto, L. Montelius, C. Mayer, C.M. Sotomayor Torres. Microelectron. Eng., submitted for publication.
[24] http://www.optics.org/article/news/8/5/14.
[25] J. Seekamp, S. Zankovych, A.H. Helfer, P. Maury, C.M. Sotomayor Torres, G. Boettger, C. Liguda, M. Eich, B. Heidari, L. Montelius, J. Ahopelto, Nanotechnology 13 (2002) 581–586.
[26] H. Schulz, H.-C. Scheer, T. Hoffmann, C.M. Sotomayor Torres, K. Pfeiffer, G. Bleidissel, G. Gruetzner, Ch. Cardinaud, F. Gaboriau, M.-C. Perpignon, J. Ahopelto, B. Heidari, J. Vac. Sci. Technol., B 18 (2000) 1861.
[27] H. Schift, L.J. Heyderman, M. Auf der Maur, J. Gobrecht, Nanotechnology 12 (2001) 173 (and references therein).
[28] F. Gottschalch, T. Hoffmann, C.M. Sotomayor Torres, H. Schulz, H.-C. Scheer, Solid-State Electron. 43 (1999) 1079.
[29] H. Schift, L.J. Heyderman, M. Auf der Mauer, J. Gobrecht, Nanotechnology 12 (2001) 173.
[30] T. Haatainen, J. Ahopelto, Phys. Scr. (in press).
[31] K. Pfeiffer, F. Reuther, M. Fink, G. Gruetzner, N. Roos, H. Schulz, H.-C. Scheer, J. Seekamp, S. Zankovych, C.M. Sotomayor Torres, I. Maximov, L. Montelius, Ch. Cardinaud, Microelectron. Eng. (submitted for application).
[32] S. Zankovych, T. Hoffmann, J. Seekamp, J.-U. Bruch, C.M. Sotomayor Torres, Nanotechnology 12 (2001) 91.
[33] Z. Yu, W. Wu, S.Y. Chou, J. Vac. Sci. Technol., B 19 (2001) 2816.
[34] M.V. Maximov, J. Seekamp, et al. (unpublished data).
[35] S. Zankovych, I. Maximov, I. Shorubalko, J. Seekamp, M. Beck, S. Romanov, D. Reuter, P. Schafmeister, A. Wiek, J. Ahopelto, C.M. Sotomayor Torres, L. Montelius, Microelectron. Eng. (submitted for publication).
[36] S.W. Pang, T. Tamamura, M. Nakao, A. Ozawa, H. Masuda, J. Vac. Sci. Technol., B 16 (1998) 1145–1149.
[37] C. Clavijo Cedeno, J. Seekamp, A.P. Kam, T. Hoffmann, S. Zankovych, C.M. Sotomayor Torres, C. Menozzi, M. Cavallini, M. Murgia, G. Ruani, F. Biscarini, M. Behl, R. Zentel, J. Ahopelto, Microelectron. Eng. 61–62 (2002) 25.
[38] M. Behl, J. Seekamp, S. Zankovych, C.M. Sotomayor Torres, R. Zentel, J. Ahopelto, Adv. Mater. 14 (2002) 588.
[39] C. Kim, M. Shtein, S.R. Forrest, Appl. Phys. Lett. 80 (2002) 4051.
[40] C. Clavijo Cedeno, A.P. Kam, C.M. Sotomayor Torres (submitted for publication).
[41] A. Lebib, S.P. Li, M. Natali, Y. Chen, J. Appl. Phys. 89 (2001) 3892.
[42] P.R. Krauss, S.P. Chou, Appl. Phys. Lett. 71 (1997) 3174.
[43] M. Austin, S.Y. Chou, J. Vac. Sci. Technol., B 20 (2002) 665.
[44] B.G. Casey, D.R.S. Cumming, I.I. Khandaker, A.S.G. Curtis, C.D.W. Wilkinson, Microelectron. Eng. 46 (1999) 125.
[45] W. Zhang, S.P. Chou, Appl. Phys. Lett. 79 (2001) 845.
[46] C. Gourgon, C. Perret, G. Micounin, Microelectron. Eng. 61–62 (2002) 385.
[47] For a report see the PHANTOMS Newsletter, May 2002 Issue 6, p23 at http://www.phantomsnet.com.
[48] S.Y. Chou, C. Keimei, J. Gu, Nature 417 (2002) 835.
[49] M. Deshmukh, et al., Appl. Phys. Lett. 75 (1999) 11.